

## СТРОИТЕЛЬНЫЕ МАТЕРИАЛЫ И ИЗДЕЛИЯ CONSTRUCTION MATERIALS AND PRODUCTS

DOI 10.22363/1815-5235-2023-19-5-534-547

UDC 624

EDN: IYOMTO

RESEARCH ARTICLE / НАУЧНАЯ СТАТЬЯ

### Effect of using 3D-printed shell structure for reinforcement of ultra-high-performance concrete

Mohammad Hematibahar<sup>1</sup> , Nikolai I. Vatin<sup>2,4</sup> , Hamid Taheri Jafari<sup>3</sup> , Tesfaldet H. Gebre<sup>4</sup> 

<sup>1</sup> Moscow State University of Civil Engineering, Moscow, Russian Federation

<sup>2</sup> Peter the Great St. Petersburg Polytechnic University, St. Petersburg, Russian Federation

<sup>3</sup> Ramsar Branch, Islamic Azad University, Ramsar, Iran

<sup>4</sup> RUDN University, Moscow, Russian Federation

✉ eng.m.hematibahar1994@gmail.com

#### Article history

Received: February 16, 2023

Revised: May 22, 2023

Accepted: June 5, 2023

#### Conflicts of interest

The authors declare that there is no conflict of interest.

#### Authors' contribution

Undivided co-authorship.

**Abstract.** This study aims to investigate the effect of 3D-printed polymer shell reinforcement on ultra-high-performance concrete. The mechanical properties of ultra-high-performance polymer reinforced concrete have been investigated. At first, the 3D-printed shell reinforcements were designed using 3D Max and Rhino 6 software. Then, each was fabricated through the fused deposition modeling method and positioned into the cubic, cylindrical, and prismatic molds. In the next step, the prepared Ultra-High-Performance Concrete mixture was poured into the molds, and the samples were cured for 28 days. Finally, the compressive, tensile, and flexural strength tests were carried out on the samples. The results indicated that the compressive, tensile, and flexural strengths of reinforced samples were lower than that of the unreinforced ones, respectively. Although including 3D-printed reinforcement decreased the mechanical properties of the Ultra-High-Performance Concrete samples, it changed the fracture mechanism of concrete from brittle to ductile.

**Keywords:** Fused Deposition Modeling, mechanical properties, fracture mechanism

#### Acknowledgements

This research was funded by the Ministry of Science and Higher Education of the Russian Federation within the framework of the state assignment No. 075-03-2022-010 dated 14 January, 2022 and No. 075-01568-23-04 dated 28 March 2023 (Additional agreement 075-03-2022-010/10 dated 09 November 2022, Additional agreement 075-03-2023-004/4 dated 22 May 2023), FSEG-2022-0010.

**Mohammad Hematibahar**, Ph.D. students, Moscow State University of Civil Engineering (National Research University), Moscow, Russian Federation; ORCID: 0000-0002-0090-5745; E-mail: eng.m.hematibahar1994@gmail.com

**Nikolai I. Vatin**, D.Sc. (Eng.), Professor of the Higher School of Industrial Civil and Road Construction, Peter the Great St. Petersburg Polytechnic University, St. Petersburg, Russian Federation; ORCID: 0000-0002-1196-8004; E-mail: vatin@mail.ru

**Hamid Taheri Jafari**, Ph.D., Researcher at Department of Civil Engineering, Ramsar Branch, Islamic Azad University, Ramsar, Iran. ORCID: 0009-0009-5816-3009; E-mail: hamidtahery2002@yahoo.co.uk

**Tesfaldet Hadgembes Gebre**, Ph.D. (Eng.), Researcher at the Department of Civil Engineering, Academy of Engineering, RUDN University, Moscow, Russian Federation; ORCID: 0000-0002-7168-5786; E-mail: tesfaldethg@gmail.com

© Hematibahar M., Vatin N.I., Hamid T.J., Gebre T.H., 2023



This work is licensed under a Creative Commons Attribution 4.0 International License  
<https://creativecommons.org/licenses/by-nc/4.0/legalcode>

#### For citation

Hematibahar M., Vatin N.I., Hamid T.J., Gebre T.H. Effect of using 3D-printed shell structure for reinforcement of ultra-high-performance concrete. *Structural Mechanics of Engineering Constructions and Buildings*.2023;19(5):534–547. <http://doi.org/10.22363/1815-5235-2023-19-5-534-547>

## Эффект от применения 3D-печатной оболочки для армирования сверхвысокопрочного бетона

М. Хематибахар<sup>1</sup>  , Н.И. Ватин<sup>2,4</sup> , Т.Д. Хамид<sup>3</sup> , Т.Х. Гебре<sup>4</sup> 

<sup>1</sup> Московский государственный строительный университет, Москва, Российская Федерация

<sup>2</sup> Санкт-Петербургский политехнический университет Петра Великого, Санкт-Петербург, Российская Федерация

<sup>3</sup> Рамсарский архитектурный университет Азад, Abass monfared Blv, Рамсар, Иран,

<sup>4</sup> Российский университет дружбы народов, Москва, Российская Федерация

✉ eng.m.hematibahar1994@gmail.com

#### История статьи

Поступила в редакцию: 16 февраля 2023 г.

Доработана: 22 мая 2023 г.

Принята к публикации: 5 июня 2023 г.

#### Заявление о конфликте интересов

Авторы заявляют об отсутствии конфликта интересов.

#### Вклад авторов

Нераздельное соавторство.

**Аннотация.** Объект исследования — это сверхвысокопрочный бетон с оболочечной 3D-печатной полимерной арматурой. Экспериментально исследованы механические свойства полимерно-армированного бетона. 3D-печатные арматурные оболочки были созданы в 3D Max и Rhino 6, изготовлены методом наплавленного осаждения и помещены в кубические, цилиндрические и призматические опалубочные формы. Экспериментально исследована прочность на сжатие, растяжение и изгиб. Прочности армированных образцов оказалась меньше, чем неармированных, но включение 3D-печатной арматуры изменило механизм разрушения бетона с хрупкого на вязкий.

**Ключевые слова:** моделирование наплавлением, механические свойства, механизм разрушения

#### Финансирование:

Исследование выполнено при финансовой поддержке Министерства науки и высшего образования РФ в рамках государственного задания № 075-03-2022-010 от 14.01.2022 г. и № 075-01568-23-04 от 28.03.2023 года (Дополнительное соглашение 075-03-2022-010/10 от 09.11.2022 г., Дополнительное соглашение № 075-03-2023-004/4 от 22.05.2023 г.), FSEG-2022-0010.

#### Для цитирования

Hematibahar M., Vatin N.I., Hamid T.J., Gebre T.H. Effect of 3D-printed shell structure on reinforcement ultra-high-performance concrete // *Строительная механика инженерных конструкций и сооружений*. 2023. Т. 19. № 5. С. 534–547. <http://doi.org/10.22363/1815-5235-2023-19-5-534-547>

## 1. Introduction

The most widely used building material in the world is concrete. Structures made of cement are more immune to environmental exposure than those built with different materials, for example, lumber or steel [1]. Concrete is used in many projects, from small ones like sidewalks and home foundations to some of the world's largest and most difficult engineering projects. Steel rebar cages are typically used to reinforce concrete and can be designed to withstand various scenarios, but their application has some restrictions. If structural elements are

**Мохаммад Хематибахар**, аспирант кафедры железобетонных и каменных конструкций, Национальный исследовательский Московский государственный строительный университет, Москва, Российская Федерация; ORCID: 0000-0002-0090-5745; E-mail: eng.m.hematibahar1994@gmail.com

**Ватин Николай Иванович**, доктор технических наук, профессор высшей школы промышленно-гражданского и дорожного строительства, Санкт-Петербургский политехнический университет Петра Великого, Санкт-Петербург, Российская Федерация; ORCID: 0000-0002-1196-8004; E-mail: vatin@mail.ru

**Хамид Тахери Джафари**, Ph.D., научный сотрудник департамента гражданского строительства Рамсарского филиала, Исламский университет Азад, Рамсар, Иран; ORCID: 0009-0009-5816-3009; E-mail: hamidtahegy2002@yahoo.co.uk

**Гебре Тесфалдет Хадгебес**, кандидат технических наук, ассистент департамента строительства инженерной академии, Российский университет дружбы народов, Москва, Российская Федерация; ORCID: 0000-0002-7168-5786; E-mail: tesfaldethg@gmail.com

details may not be sufficient to withstand severe impact like seismic or blast loading. In addition, pouring concrete into rebar cages with high reinforcing bar ratios is challenging and takes a lot of time and effort. Steel reinforcement is also costly and has a significant carbon footprint [2]. Utilizing fibers is yet another method for enhancing the properties of cementitious composites [3–10]. However, controlling how the fibers in fiber-reinforced composites are distributed isn't easy. Furthermore, fiber orientation is affected by execution boundaries, for example, the size of the underlying member and the bearing of the substantial stream during projecting [11].

An alternative method for creating intricate geometries that can be used as reinforcement in concrete has recently emerged. Small and large-scale fabrication of three-dimensional elements from various materials is made possible by the additive manufacturing (AM) process, which is also referred to as "3D printing" [12–14]. Thanks to recent advancements [15], complex geometries can now be created for polymers using 3D printing techniques like Fused Deposition Modeling (FDM). The digitally controlled processes by which material is joined to create a new object are the foundation of 3D printing. Low costs, safety, the ability to print aesthetically pleasing structures in any design, and minimizing environmental impact are just a few benefits of 3D construction printing [16]. For instance, the reinforcing Cementitious Backfill Composite (CBC) with a variety of 3D Printed Polymeric Lattice (3D-PPL) shapes increases its ductility [17]. The researchers used the digital image correlation technique and found that 3D-PPL can make CBC's brittle behavior ductile without affecting its hardening properties. Farina and others [18] carried out Three Point Bending Tests (TPBT) on a cement mortar reinforced with polymeric and metallic 3D-printed fibers with various surface morphology and roughness. It was claimed that samples reinforced with fibres with a high surface roughness had a stronger interfacial connection compared to samples that were left unreinforced and samples reinforced with smooth fibres.

Another uniform testing technique was introduced in view of consolidated Twist Hub force (TORAX) test for accurate reflection of mechanical properties of 3D-printed cement and mortar [19]. It was discovered that 3D-printed concrete lacks the characteristics of cast concrete because the shear stress is only transferred through the adhesive properties of the cement matrix. The three distinct types of fibers (carbon, glass, and basalt) were used to reinforce 3D-printed concrete and various tests were conducted on the fiber-reinforced specimens [20]. It was found that the samples' flexural performance was significantly improved by a 1 % volumetric fraction of carbon fibers aligned along the printing direction. In contrast, glass and basalt fibers had no effect. The results also showed that the improved combination's flexural and compressive strength rises up to 30 and 80 MPa respectively. Different authors showed that 3 percent by volume of carbon fibers with a length of 3 millimeters can significantly increase the flexural strength of concrete up to 120 MPa [21]. Similarly, a study shows that 3D-printable Ultra-High-Performance Concrete (UHPC) had a lower compressive strength (32–56 %) than mold-cast UHPC [22].

Printed specimens may have a compressive strength of up to 22 % lower than those placed in molds [23]. In a previous study, the mechanical characteristics of high-performance printing concrete with steel fibre reinforcement of varied lengths and volume contents were examined [24]. It was found that printed concrete had lower compressive and flexural strengths than the cast concrete. As such, the compressive and flexural qualities of printed concrete were in the range of 70–111 MPa and 6–15 MPa, respectively, while the compressive and flexural qualities of cast concrete were 90–113 MPa and 11–14 MPa. The steel fiber orientation distribution in 3D-printed UHPC is quantitatively investigated [25]. According to this, the fibre alignment parallel to the printing direction was greatly enhanced by the large fibre volume percentage. The mechanical performance of the printed specimens was superior to that of the mold-cast ones because of this fiber alignment. Various spatial distributions of 3D-printed fibers were analyzed to show how reinforcement orientation and distribution affected created reinforcement networks of interconnected photopolymer resin fibers [26]. Subsequently, it was shown that when a triangulated reinforcing structure with a denser mesh was utilized in places with higher tensile stresses, the peak flexural strength rose. However, they were unable to observe the ductile behavior in the samples because it only utilised a small percentage of polymer reinforcement in their studies. The study improved the cementitious material's performance by using bio-inspired polymeric structures that were 3D-printed as reinforcement for cement mortar [27]. The impact of 3D-printed spatial support on flexural properties of conventional mortar was studied [28]. The study discovered that the flexural behavior of specimens is significantly affected by the shape and size of a spatial 3D-printed element.

However, concrete's Modulus of Elasticity (ME) and Energy Absorption Capacity (EAC) are two crucial deformation parameters. ME is an important parameter in the design of concrete structures because it shows the material's resistance to deformation under load. ME of concrete is a good indicator of strength because it

measures the stiffness of the concrete. The concrete is more rigid the higher the ME value. ME is influenced by various factors, including the concrete's density, moisture content, the Interfacial Transition Zone (ITZ) thickness, mixture homogeneity, reinforcement material, cement matrix, bonding between aggregates, and porosity in each part. EAC measures the material's capacity to absorb energy during deformation. Particularly in locations where concrete structures are subjected to frequent loads and seismic activity, the energy-absorbing properties of concrete can beneficially reduce the likelihood of their failure. In addition, impact loads must be protected against important infrastructure buildings, such as nuclear power plants and smaller technical facilities, as failure can result in significant damage. Thus, common fields are interested in a suitable structure material with an extraordinary energy retention limit.

As previously stated, there is a lot of interest in utilizing AM methods to create reinforcing elements that conventional steel cages or fibers could replace. Despite these efforts, additional research is required to strengthen concrete using 3D printing. A novel approach to strengthening concrete was utilized in this study by using 3D printing technology. The present study uses 3D-printed shell Polylactic Acid (PLA) structures as UHPC reinforcements, focusing on a unique class of composites. It examined the fracture characteristics, deformation parameters, and mechanical features like compressive, tensile, and flexural strengths of UHPC reinforced with 3D-printed PLA shells. Using FDM, a popular 3D printing technique, the reinforcement was created in the shape of a shell.

## 2. Methods, Materials, and Sample Preparation

**2.1. Methods.** Even though 3D-printing concrete has received the most attention in civil engineering, there has recently been a lot of interest in 3D-printing reinforcements. The mechanical properties (such as compressive, tensile, and flexural strengths), as well as the fracture mechanism of various samples, were analyzed in this paper after UHPC was reinforced with 3D-printed PLA. The approach taken in this study is depicted in Figure 1. The 3D-printed reinforcement shells were initially plotted using 3D Max and Rhino 6 software. The FDM process produced the PLA materials, which were then inserted into the molds. The samples were cured after the UHPC mixture was poured into the molds in the subsequent step. The samples were then subjected to various tests, and the results were examined and discussed.

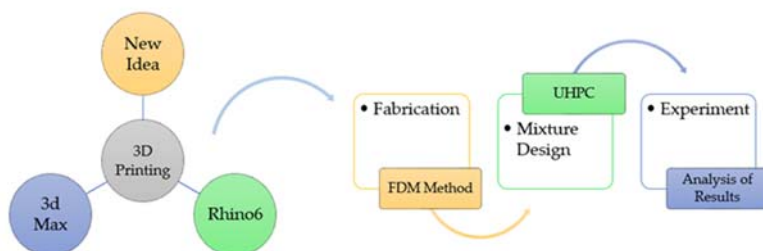


Figure 1. The methodology of the current study



Figure 2. Design of shell reinforcement

The 3D Max and Rhino 6 software were utilized to design the shell reinforcement. The concept was initially created in 3D Max before being completed using the architectural software Rhino 6. The honeycomb openings were provided on the shell surface to allow concrete mixture penetrate through them before its setting. In addition, Figure 2 shows how the concrete mixture can adhere appropriately to the shell surface and fill these holes. These honeycombs were chosen to be small enough to be incorporated into the shell surface and to allow the concrete mix to flow readily through it. Honeycombs are made topologically by connecting regular or random polygons with a specific thickness in a plane. The honeycomb structure has the advantages of simplicity, high porosity, lightweight, and simple manufacturing, all indicating high impact resistance potential.

In most cases, structures use honeycomb or honeycomb-like shells as their core to increase their capacity for carrying loads and absorbing energy. As a result, it is necessary to investigate the mechanical properties of honeycombs or honey-comb-composed composite structures under various loading conditions. In addition, one of the goals of using UHPC is to reduce the amount of cement and CO<sub>2</sub> emissions required for a particular load [29]. As a result, utilizing a reinforcement strategy with a significant non-cementitious volume fraction can also

significantly enhance this advantage. The ongoing review examines UHPC’s behavior, supported with a 3D-printed honeycomb PLA shell structure under compressive, tensile, and flexural loads.

Three samples were taken into consideration for each of the compressive and tensile tests. Two of the samples were reinforced using the 3D-printing method, and one of the samples was unreinforced concrete. The first reinforced 3D-printed sample had more honeycomb holes at the shell’s top, while the second sample had more honeycomb holes at its bottom. The purpose of considering this modification to the arrangement of the holes was to investigate the effect of the bonding that existed between the aggregates and the cement matrix in the 3D-printed shell structure. The proper movement of the concrete mixture through these holes required consideration of various hole sizes. For flexural tests, two examples were considered. One was unreinforced, and another was built up using a 3D-printing technique.

The thickness of the shells was 2 cm, and their dimensions were  $8 \times 8 \times 8 \text{ cm}^3$  for compressive,  $8 \times 8 \times 13 \text{ cm}^3$  for tensile, and  $58 \times 8 \times 8 \text{ cm}^3$  for flexural strength tests, as shown in Figure 3.

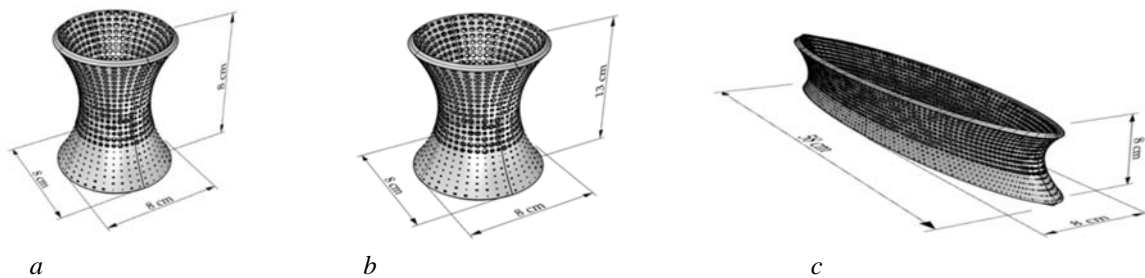


**Figure 3.** Dimensions of shell reinforcements for: *a* — compressive; *b* — tensile; *c* — flexural strength tests

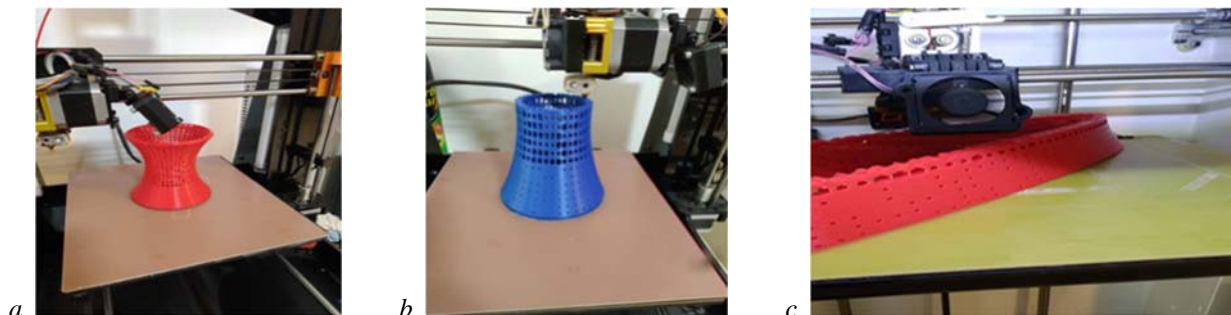
PLA material was printed using the FDM 3D-printing method to create concrete reinforcement. This study chose PLA because of its appropriate mechanical properties, such as its excellent printability, mechanical properties, and environmental friendliness. Because being reinforced with a polymeric substance rather than steel, polymer-reinforced constructions are stronger, lighter, and more thermally insulated [30]. Table 1 shows the mechanical properties of PLA. PLA reinforcement meshes were made using Quantum, a commercially available FDM 3D-printer. The model is printed layer by layer, bottom to top, using FDM. The printing parameters may affect the final structure’s mechanical characteristics. As a result, they remained constant throughout this investigation. At 60 °C for the build platform and 190 °C for the extruder, all parts were printed with identical parameters. The stress transfer and, ultimately, the sample’s overall mechanical characteristics may be impacted by the specified printing path, which substantially impacts the mechanical behavior of printed reinforcements.

Figure 4 shows the process of fabricating 3D-printed reinforcements. The shell formation is constructed layer by layer using 3D-printed PLA materials. Figure 5 demonstrates the completed forms of the shells.

Table 1

The mechanical properties of PLA [31]

| Material | Ultimate Tensile Strength, MPa | Yield Strength, MPa | Maximum Strain, % |
|----------|--------------------------------|---------------------|-------------------|
| PLA      | $57.16 \pm 0.35$               | $52.47 \pm 0.35$    | $2.35 \pm 0.05$   |



**Figure 4.** The 3D-printing process of reinforcements for: *a* — compressive; *b* — tensile; *c* — flexural strength tests



**Figure 5.** The completed 3D-printed shells for:  
a — compressive; b — tensile; c — flexural strength tests

**2.2. Materials and Sample Preparation.** Ordinary Portland Cement (OPC) from Sabzevar factory, Sabzevar, Iran, micro silica manufactured by Novolipetsk Company (NLMK), Novolipetsk, Russia, quartz sand (as fine aggregates), crushed granite (as coarse aggregates) superplasticizer and tap water were used to prepare concrete samples. The OPC compositions are depicted in Table 2. It should be noted that the initial and final setting time of the OPC was 30 and 600 min, respectively. Besides, due to its micro-filling property, microsilica was used to fill the voids between the 3D-printed structure and the cementitious matrix [32; 33]. Table 3 presents the chemical constituents of microsilica. Fine aggregates with a specific gravity of 2.38 and coarse aggregates with a specific gravity of 2.65 were collected from the Semnan region, Iran. Figure 6 shows the gradation curves of fine and coarse aggregates.

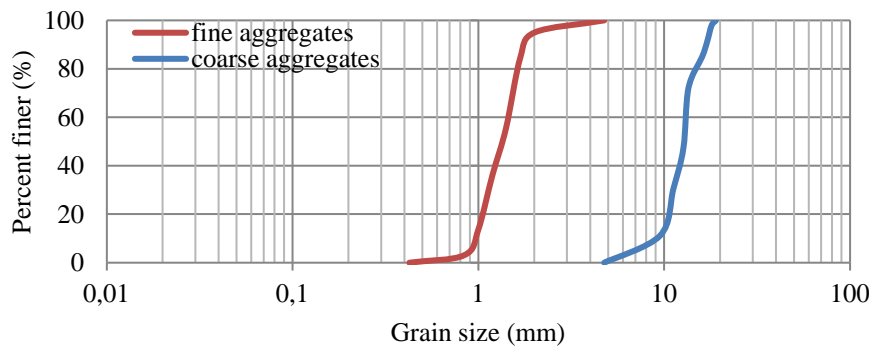


**Figure 6.** Gradation curves of fine and coarse aggregates

Table 2

**Chemical composition of OPC**

| Oxide, %         |                                |      |                 |                                |       |                  |        | Blaine, m <sup>2</sup> /kg | Specific Gravity |
|------------------|--------------------------------|------|-----------------|--------------------------------|-------|------------------|--------|----------------------------|------------------|
| SiO <sub>2</sub> | Fe <sub>2</sub> O <sub>3</sub> | MgO  | SO <sub>3</sub> | Al <sub>2</sub> O <sub>3</sub> | CaO   | K <sub>2</sub> O | L.O.I. |                            |                  |
| 19.52            | 4.04                           | 4.36 | 2.89            | 4.81                           | 62.18 | 0.6              | 1.62   | 387                        | 3.14             |

The UHPC was selected in this study as the concrete material due to its superior strength to normal concrete. Although UHPC has been commercially available for over a decade, the knowledge of its use in 3D-printing is just beginning to become more widely available. UHPC is more brittle than normal concrete, and thus it may be expected to be more difficult to improve its ductility using 3D-printed reinforcement. It is, therefore, necessary to investigate whether the same degree of ductility improvement can be obtained in UHPC as in normal concrete or not. The water/cement ratio was 0.25 in the preparation of this type of concrete, according to the suggestion of Chen et al. [34]. Besides, the micro silica to cement percentage was selected to be 15 %, as it was the optimum percentage based on paper [35]. Table 4 shows the mixture design of UHPC in the present research.

Table 3

**Chemical composition of micro silica**

| Chemical Composition                         | Value, % |
|--|----------|
| Silicon dioxide (SiO <sub>2</sub> )          | 90–92    |
| Alumina (Al <sub>2</sub> O <sub>3</sub> )    | 0.68     |
| Iron oxide (Fe <sub>2</sub> O <sub>3</sub> ) | 0.69     |
| Calcium oxide (CaO)                          | 1.58     |
| Magnesium oxide (MgO)                        | 1.01     |
| Sodium oxide (Na <sub>2</sub> O)             | 0.61     |
| Potassium oxide (K <sub>2</sub> O)           | 1.23     |
| Carbon (C)                                   | 0.98     |
| Sulfur (S)                                   | 0.26     |

The mentioned materials were mixed using a pan mixer at a constant rate of 48 rpm. For this purpose, aggregates were mixed with each other for about 2 min. Then, water, cement, silica fume, and superplasticizer were added and mixed until a homogeneous mix was achieved. Next, the molds were polished with oil, and the 3D-printed shell reinforcements were positioned inside them. For cylindrical samples, molds with diameters of 100 mm and heights of 200 mm were applied. Moreover, for cubic and prismatic samples, molds with dimensions of  $100 \times 100 \times 100 \text{ mm}^3$  and  $600 \times 100 \times 100 \text{ mm}^3$  were utilized, respectively (Figure 7). The prepared mixture was poured into the molds (Figure 8). The samples were placed in a water tank at a temperature of about  $20 \text{ }^\circ\text{C}$  to cure the concrete specimens (Figure 9). After curing for 28 days, 3D-printed reinforced UHPC samples were tested for determination of their compressive, flexural, and tensile strengths based on Russian State Standard GOST 10180-2012 “Concretes”<sup>1</sup>, Standard Test Method for Flexural Strength of Concrete ASTM C293/C293M<sup>2</sup>, and ASTM C496<sup>3</sup>, respectively.

Table 4

Mixture design of UHPC

| Material | Cement, $\text{kg/m}^3$ | Micro silica, $\text{kg/m}^3$ | Sand, $\text{kg/m}^3$ | Gravel, $\text{kg/m}^3$ | Superplasticizer, $\text{kg/m}^3$ | Water, $\text{kg/m}^3$ |
|----------|-------------------------|-------------------------------|-----------------------|-------------------------|-----------------------------------|------------------------|
| UHPC     | 420                     | 65                            | 945                   | 635                     | 105                               | 105                    |

Figure 7. Concrete molds: *a* — cube; *b* — cylinder; *c* — prism

### 3. Results and Discussion

**3.1. Compressive Strength.** Table 5 presents the compressive strength values of the samples. As seen from the table, the unreinforced sample had the maximum compressive strength value.

Table 5

Compressive strength values

| Specimen               | Unreinforced sample | First reinforced sample | Second reinforced sample |
|------------------------|---------------------|-------------------------|--------------------------|
| Ultimate Strength, MPa | 36                  | 33.2                    | 27.5                     |

As shown in Figure 8, the compressive properties of the 3D-printed reinforced UHPC were lower than those of the unreinforced concrete. Nonetheless, it showed a more expanded elaxation curve.

There may be various reasons why 3D-printed reinforced specimens have a lower compressive strength than unreinforced specimens. One reason is the existence of weak boundary connections between concrete and 3D-

<sup>1</sup> GOST10180 Concretes. Methods for Determination of Strength by Control Samples. Standartinform: Moscow, Russia. 2013. (In Russ.) <https://docs.cntd.ru/document/1200100908> (accessed: 14.03.2023).

<sup>2</sup> ASTM C293/C293M-16 Standard Test Method for Flexural Strength of Concrete (Using Simple Beam with Center-Point Loading). American Society for Testing of Materials: West Conshohocken PA USA 2016.

<sup>3</sup> ASTM C496 Standard Test Method for Splitting Tensile Strength of Cylindrical Concrete Specimens. American Society for Testing of Materials: West Conshohocken PA USA, 2017.

printed reinforcement. Compared to the unreinforced sample, this may result in material fracture under compression at lower stress levels. Printed reinforcement may introduce numerous interfacial zones between the matrix and reinforcement, facilitating the crack initiation in reinforced specimens. In addition, the spacing regions of the printed reinforcement make matrix compaction slightly more challenging in the reinforced specimens, possibly resulting in more imperfections than in the unreinforced specimens. One more justification for the lower strength of reinforced specimens in comparison with the unreinforced one might be because of the weak bond between the reinforcement surface and the cement.

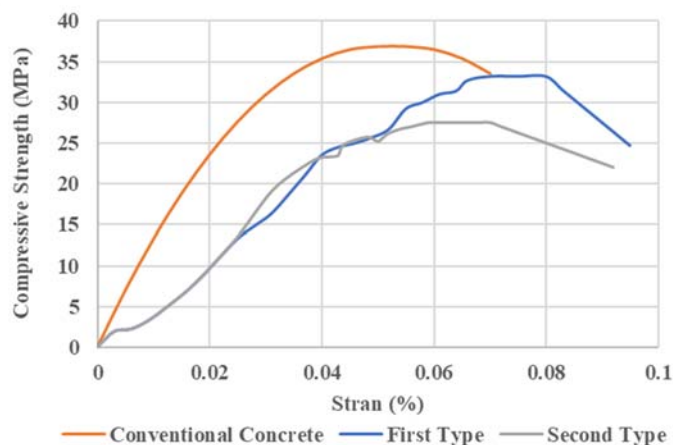


**Figure 8.** Variation of compressive stress with strain for cubic samples

It should be noted that the printed shell exhibited only natural roughness because no specific measures were taken to improve the bond in the tests. However, if necessary, printing the reinforcement with a specific surface roughness and morphology will undoubtedly increase the bond significantly. In previous research, it was also found that reinforced samples had a lower compressive strength. Salazar et al., for example [29] utilized 3D-printed polymeric lattices made of either Acrylonitrile Butadiene Styrene (ABS) or PLA to reinforce UHPC. Their findings demonstrated that the reinforced sample had a lower compressive strength than the unreinforced sample. The strength was decreased because less of the high compressive-modulus UHPC was incorporated into the specimens due to using lattice reinforcement.

In contrast to the unreinforced sample, the reinforced sample's core did not yield, and only the cover was separated from the reinforced portion, as shown in Figure 9. The 3D-printed reinforcement had the possibility to help the center of the specimen. In addition, the first reinforced sample had a stronger connection to the cementitious matrix than the second. In the first reinforced specimen, because the lower part of the support has fewer openings, most of the aggregates are in the center and inside the shell. However, additional holes are at the bottom of the reinforcement in the second case. As a result, most of the aggregates will be found in the center of the sample because the concrete was poured through the holes. Consequently, the strength will be greater if more aggregates are in the sample center.



**Figure 9.** Sample after compression tests:  
*a* — unreinforced; *b* — first reinforced; *c* — second reinforced

**3.2. Tensile Strength.** Because the printed PLA shell in reinforced specimens constitutes a part of the cross-section in tension tests, Table 6 demonstrates that the unreinforced sample has the highest tensile strength value of all the samples. As a result, reinforced specimens have a lower tensile strength because the matrix's actual cross-section area is smaller than the unreinforced specimen. In addition, because the reinforced specimens were shaken externally to eliminate internal air bubbles and evenly distribute the mixture throughout the mold, the reinforced sample has less compaction than the unreinforced specimen. Be that as it may, for the unreinforced example, the mixture layers were compacted with steel bars. Other possible explanations for the higher tensile strength of the unreinforced specimen in comparison to the reinforced ones include the printed reinforcement's higher geometrical variability and less homogenous microstructure.

Table 6

**The values of tensile strength**

| Specimens             | Unreinforced sample | First reinforced sample | Second reinforced sample |
|-----------------------|---------------------|-------------------------|--------------------------|
| Tensile strength, MPa | 5.49                | 4.11                    | 2.86                     |

The unreinforced specimen split into two different fragments, as depicted in Figure 10. The fragments demonstrate the brittle nature of the unreinforced specimen, which fractures catastrophically and without warning. However, because the reinforcement was 3D-printed, the reinforced samples' cores remained intact, only the concrete cover failed. In other words, when subjected to tension, the unreinforced specimen displayed the typical brittle behavior of cementitious materials. It only developed one crack and has a low strain capacity. However, specimens reinforced with a 3D-printed PLA shell can withstand greater strains. The concrete samples' ductility significantly increased due to the 3D-printed PLA reinforcement's ability to prevent complete splitting. It very well may be likewise seen that a single shear plane developed in the unreinforced specimen.



**Figure 10.** Sample after tension tests:  
*a* — unreinforced; *b* — first reinforced; *c* — second reinforced

In contrast, reinforced specimens contained many longitudinal cracks oriented parallel or nearly parallel to the external tensile stresses near the failure zone. Cementitious composites' deflection and tensile strain capacity were significantly increased when PLA reinforcement was used compared to the control specimen. Zhang et al.'s findings are consistent with this finding [36]. By conducting Brazilian splitting tests, it was demonstrated that 3D-PP reinforced cemented tailings backfill (CTB) samples have higher strains. In addition, the study discovered that adding 3D-PP effectively mitigates the damage process inherent in conventional CTB and enhances the strength property of the backfill. In another review, Mechtcherine et al. [37] also showed that the tensile strength of 3D-printed steel bars was about 20 % lower than that of conventional reinforcement bars. However, 3D-printed steel bars outperformed conventional bars in terms of yielding and strain capacity.

**3.3. Flexural Strength.** Figure 11 shows the variation of flexural stress with strain for prismatic samples. As seen from the figure, the inclusion of 3D-printed reinforcement does not fundamentally alter the behavior of the UHPC prior to the maximum stress, but it significantly enhances the post-cracking behavior of UHPC. The conventional concrete had linear behavior, while the reinforced concrete had nonlinear behavior. Figure 12 shows that the deformation of the reinforced was more than conventional concrete.

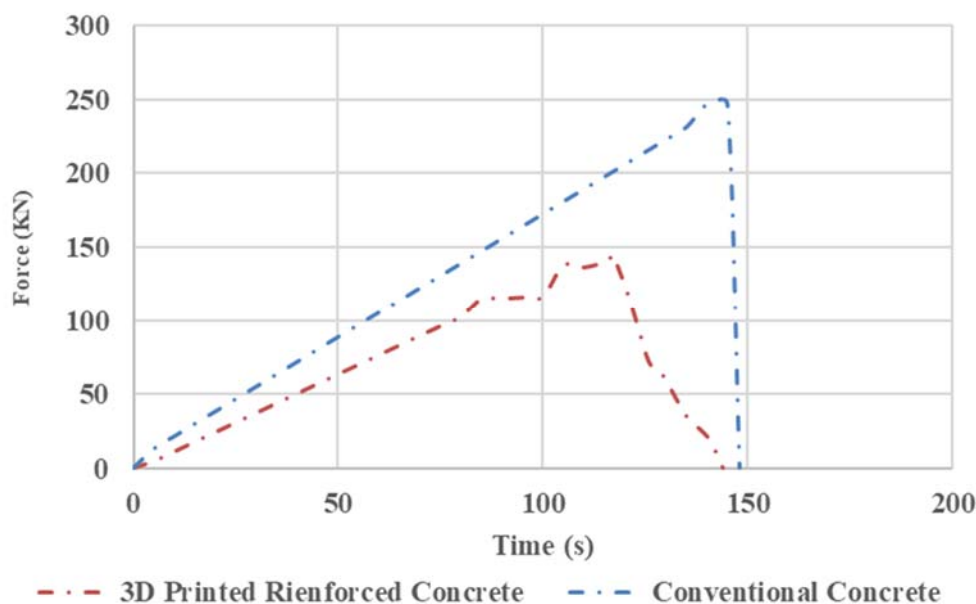


Figure 11. Variation of flexural stress with strain for prismatic samples

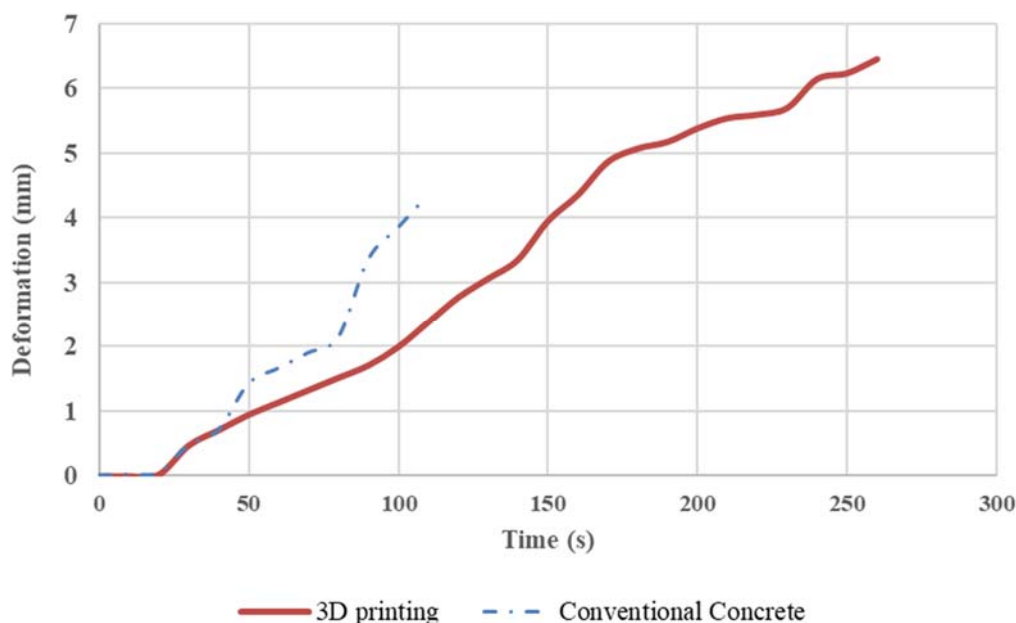


Figure 12. The deformation versus curve

The flexural strength of the unreinforced sample was greater than that of the 3D-printed reinforcement sample, as shown in Table 7. Compared to the unreinforced sample, the neutral axis of the reinforced sample is shifted closer to the sample's top side due to the reinforcement's lower elastic modulus than the cementitious matrix. Consequently, the reinforced sample's bottom side will experience higher tensile stress at the same bending moment. Likewise, because the reinforced specimen might contain imperfections, for example, trapped air voids because of poorly performed vibration, the flexural resistance strength in the unreinforced specimen is generally higher than the reinforced one. Similarly, Le et al. [38] demonstrated that 3D-printed reinforcement had lower strength values (compressive strength of 75–102 MPa and flexural strength of 6–17 MPa). In contrast, unreinforced concrete had high strengths (107 MPa in compression and 11 MPa in bending).

The values of flexural strength

| Specimens              | Unreinforced sample | Reinforced sample |
|------------------------|---------------------|-------------------|
| Flexural Strength (KN) | 248                 | 147               |

Figure 13 demonstrates the failure of an unreinforced prismatic sample. The failure of this sample during the flexure test was immediate. The sample was broken into two parts after cracks appeared as the load increased. In other words, it showed classic brittle material behavior. The fracture was catastrophic and sudden at low deformation, with failure characterized by one full-depth crack near the center of the beam.

The gradual failure of the 3D-printed reinforcement sample is shown in Figure 14. There was a time lag between the cracks appearing and the sample failure. On the sample's surface, the crack propagation can be seen. The crack had a narrow width at the start of the loading. The cracks spread throughout the sample and got wider as the loading progressed. As it moved toward the compression zone, the numerous cracks widen in the tension zone. The observed cracks begin in the middle of the beam's span and move upward. The bottom of the reinforced specimen experiences significant tensile stresses during the flexural process. Cracks will appear when the material reaches its tensile strength. One of the multiple cracks eventually becomes the dominant crack, significantly decreasing the sample's load capacity. The failure occurred in the reinforced specimen without the sample collapsing, making it challenging to distinguish the two sections from one another. This response clearly demonstrates that the reinforcement significantly altered the brittle cracking failure of cementitious mortar to ductile failure. Cracking and tortuous crack paths are associated with the ductility-enhancing mechanisms that occur during bending. 3D-printed shell can restrict the spread of breaks and give the concrete, effective resistance against more intense loadings after the presence of breaks (Figure 15). The findings are consistent with those of previous investigations. Salazar and others [29] stated that the 3D-printed reinforcement successfully converted the UHPC's brittle behavior into a ductile one. Mechtcherine and others [37] demonstrated that using 3D-printed steel bars in concrete enhanced ductility and strain capacity compared to conventional bars. Farina and others [18] concluded that the unreinforced specimens fail brittlely and have no residual strength after the crack has begun.

In contrast, specimens reinforced with polymeric and metallic 3D-printed fibers demonstrated residual load carrying capacity. Flexural studies by Xu and Šavija [1] revealed that unreinforced specimens displayed a brittle response with a comparatively modest deflection at failure. Then again, all specimens built up with 3D-printed polymeric lattices could withstand considerably higher displacement. Xu et al. [39] utilized 3D-printed polymeric octet cross-section structures to reinforce cementitious composites and noted higher flexibility compared to the unreinforced test.



Figure 13. Unreinforced sample after failure

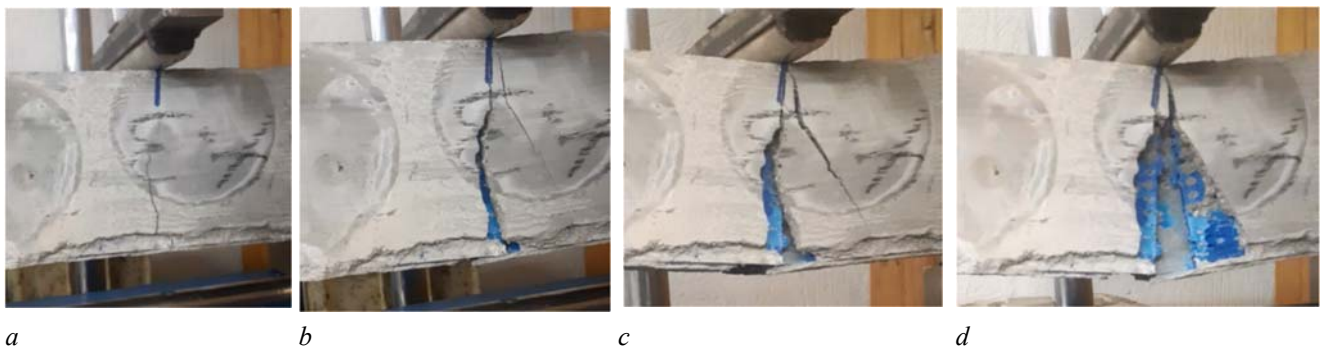


Figure 14. 3D-printed reinforced sample:

*a* — cracking moment; *b* — crack propagation; *c* — appearance of more cracks; *d* — failure

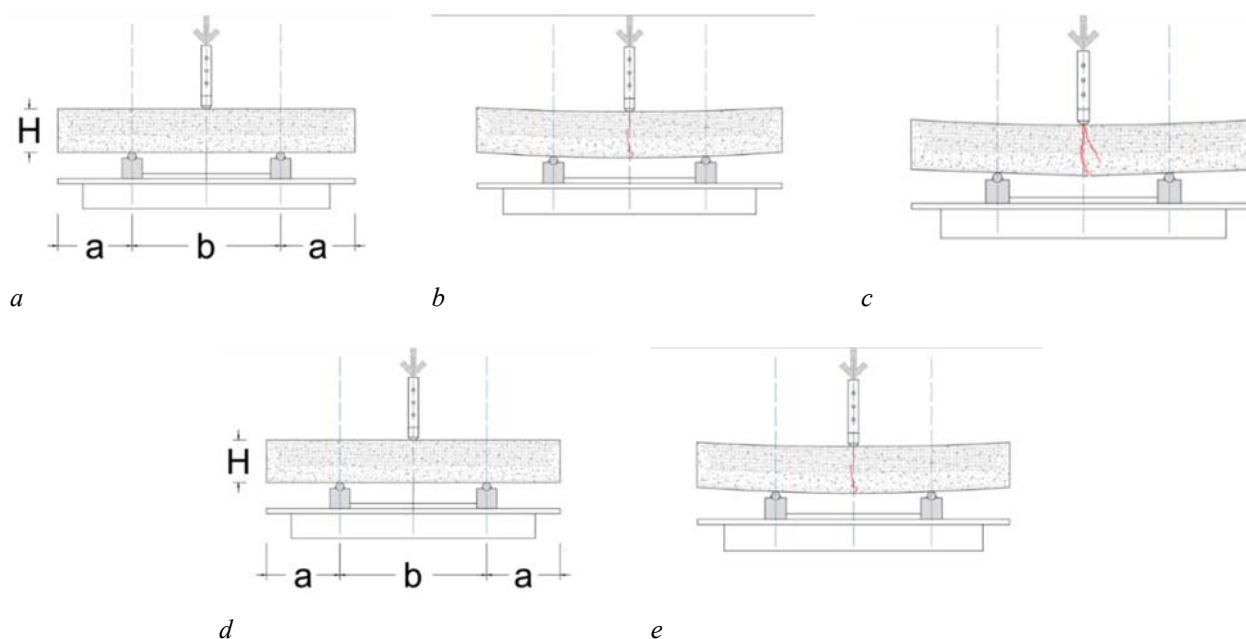


Figure 15. The 3D-printed reinforcement specimen failure mode

#### 4. Conclusions

The main goal of the current study was to improve the mechanical properties and fracture mechanism of concrete by using 3D-printed reinforcement instead of steel bars, etc. For this purpose, the compressive, tensile, and flexural strength values of different 3D-printed reinforcement and unreinforced samples were determined and analyzed. The achieved findings of this research can be summarized as follows:

1. The UHPC samples with 3D-printed reinforcements showed poor mechanical properties compared to the unreinforced ones. The compressive, tensile, and flexural strengths of reinforced samples were less than those of unreinforced.

2. The reinforced samples indicated ductile behavior, while the behavior of the unreinforced samples was brittle. In other words, although the 3D-printed samples had weaker mechanical properties than the unreinforced ones, they could carry a load even after failure. The weakness of 3D-printed polymer reinforcement can be they by creating a very complicated spatial shape with artificially created roughness of its surfaces. Such spatial reinforcement, the creation of which is not possible using steel bars, would match the strength properties of steel cages.

3. The fracture mechanism of concrete improved by using 3D-printed reinforcement. The ductility of UHPC can be efficiently increased with 3D-printed reinforcement made from PLA, which is widely utilized in AM and is available at a reasonable cost.

4. The current study presents a new method for reinforcing concrete. The obtained results prove that 3D-printing can convert ideas into reality.

Hence, it can be concluded that using a 3D-printed honeycomb PLA shell structure as reinforcement in concrete results in energy absorption improvement, weight reduction, and good symmetry. It should be noted that the polymer required for a 3D-printer can also be obtained from waste polymers. Utilization of large amounts of recycled polymer for 3D-printed reinforcements would be advantageous in terms of both the construction industry and environmental protection. Furthermore, it allows to control the reinforcement distribution within a structure precisely.

#### References

- Xu Y., Šavija B. Development of strain hardening cementitious composite (SHCC) reinforced with 3D printed polymeric reinforcement: Mechanical properties. *Composites Part B: Engineering*. 2019;(174):107011. <https://doi.org/10.1016/j.compositesb.2019.107011>

2. Jaimes W., Maroufi S. Sustainability in steel making. *Current opinion in green and sustainable chemistry*. 2020; (24):42–47. <https://doi.org/10.1016/j.cogsc.2020.01.002>
3. Hasanzadeh A., Vatin N.I. Hematibahar M., Kharun M. Shooshpasha I. Prediction of the mechanical properties of basalt fiber reinforced high-performance concrete using machine learning techniques. *Materials*. 2022;(15):7165. <https://doi.org/10.3390/ma15207165>
4. Ji Y., Xu W., Sun Y., Ma Y., He Q., Xing Z. Grey correlation analysis of the durability of steel fiber-reinforced concrete under environmental action. *Materials*. 2022;(15):4748. <https://doi.org/10.3390/ma15144748>
5. Mu Y., Xia H., Yan Y., Wang Z., Guo R. Fracture behavior of basalt fiber-reinforced airport pavement concrete at different strain rates. *Materials*. 2022;(15):7379. <https://doi.org/10.3390/ma15207379>
6. Mohtasham Moein M., Saradar A., Rahmati K., Shirkouh A.H. Sadrinejad I., Aramali V., Karakouzian, M. Investigation of impact resistance of high-strength portland cement concrete containing steel fibers. *Materials*. 2022;(15): 7157. <https://doi.org/10.3390/ma15207157>
7. Eskandarinia M., Esmailzade M., Hojatkashani A., Rahmani A., Jahandari S. Optimized alkali-activated slag-based concrete reinforced with recycled tire steel fiber. *Materials* 2022(15):6623: <https://doi.org/10.3390/ma15196623>
8. Hematibahar M., Vatin N.I., Alaraza H.A.A., Khalilavi A., Kharun M. The prediction of compressive strength and compressive stress–strain of basalt fiber reinforced high-performance concrete using classical programming and logistic map algorithm. *Materials* 2022;19:6975. <https://doi.org/10.3390/ma15196975>
9. Hasanzadeh A., Shooshpasha I. A study on the combined effects of silica fume particles and polyethylene terephthalate fibres on the mechanical and microstructural characteristics of cemented sand. *International Journal of Geosynthetics and Ground*. 2021;(7):98. <https://doi.org/10.1007/s40891-021-00340-4>
10. Hasanzadeh A., Shooshpasha I. Influences of silica fume particles and polyethylene terephthalate fibers on the mechanical characteristics of cement-treated sandy soil using ultrasonic pulse velocity. *Bulletin of Engineering Geology and the Environment*. 2022;(81)14. <https://doi.org/10.1007/s10064-021-02494-x>
11. Stähli P., Van Mier J.G. Manufacturing fibre anisotropy and fracture of hybrid fibre concrete. *Engineering Fracture Mechanics*. 2007;(74):223–242. <https://doi.org/10.1016/j.engfracmech.2006.01.028>
12. Kim T.G., Shin G.Y., Shim D.S. Study on the interfacial characteristics and crack propagation of 630 stainless steel fabricated by hybrid additive manufacturing (additional DED building on L-PBFed substrate). *Materials Science and Engineering*. 2022;(835):142657. <https://doi.org/10.1016/j.msea.2022.142657>
13. Ning X., Liu T., Wu C., Wang C. 3D printing in construction: current status implementation hindrances and development agenda. *Advances in Civil Engineering*. 2021;(2):6665333. <https://doi.org/10.1155/2021/6665333>
14. Tan W., Wang P. Experimental study on seepage properties of jointed rock-like samples based on 3D printing techniques. *Advances in Civil Engineering*. 2020:9403968. <https://doi.org/10.1155/2020/9403968>
15. Boparai K.S., Singh R., Singh H. Development of rapid tooling using fused deposition modeling: a review. *Rapid Prototyping Journal*. 2016;(22):281–299. <https://doi.org/10.1108/RPJ-04-2014-0048>
16. Mansouri A., Binali A., Aljawi A., Alhammad A., Almir K., Alnuaimi E., Alyousuf H., Rodriguez-Ubinas E. Thermal modeling of the convective heat transfer in the large air cavities of the 3D concrete printed walls. *Cogent Engineering*. 2022;9(1):2130203. <https://doi.org/10.1080/23311916.2022.2130203>
17. Qin S., Cao S., Yilmaz E., Li J. Influence of types and shapes of 3D printed polymeric lattice on ductility performance of cementitious backfill composites. *Construction and Building Materials*. 2021;307:124973. <https://doi.org/10.1016/j.conbuildmat.2021.124973>
18. Farina I., Fabbrocino F., Carpentieri G., Modano M., Amendola A., Goodall R., Feo L., Fraternali F. On the reinforcement of cement mortars through 3D printed polymeric and metallic fibers. *Composites Part B: Engineering*. 2016;(90): 76-85. <http://doi.org/10.1016/j.compositesb.2015.12.006>
19. Meurer M., Classen M., Mechanical properties of hardened 3D printed concretes and mortars-development of a consistent experimental characterization strategy. *Materials*. 2021;14(4):752. <https://doi.org/10.3390/ma14040752>
20. Hambach M., Volkmer D. Properties of 3D-printed fiber-reinforced portland cement paste. *Cement and Concrete Composites*. 2017;79:62–70. <https://doi.org/10.1016/j.cemconcomp.2017.02.001>
21. Hambach M., Möller H., Neumann T., Volkmer D. Portland cement paste with aligned carbon fibers exhibiting exceptionally high flexural strength (>100MPa). *Cement and Concrete Research*. 2016;89:80–86. <https://doi.org/10.1016/j.cemconres.2016.08.011>
22. Medicis C., Gonzalez S., Alvarado Y.A., Vacca H.A., Mondragon I.F., Garcia R., Hernandez G. Mechanical performance of commercially available premix UHPC-based 3D printable concrete. *Materials*. 2022;15:6326. <https://doi.org/10.3390/ma15186326>
23. Rehman A.U., Kim J.H. 3D Concrete printing: A systematic review of rheology mix designs mechanical microstructural and durability characteristics. *Materials*. 2021;(14):3800. <https://doi.org/10.3390/ma14143800>
24. Pham L., Tran P. Sanjayan J. Steel fibres reinforced 3D printed concrete: influence of fibre sizes on mechanical performance. *Construction and Building Materials*. 2020;(250):118785. <https://doi.org/10.1016/j.conbuildmat.2020.118785>
25. Arunothayan A.R., Nematollahi B., Ranade R., HauBong S., Sanjayan J.G., Khayat K.H. Fiber orientation effects on ultra-high performance concrete formed by 3D printing. *Cement and Concrete Research*. 2021;(143):106384. <https://doi.org/10.1016/j.cemconres.2021.106384>

26. Nam Y.J., Hwang Y.K., Park J.W., Lim Y.M. Feasibility study to control fiber distribution for enhancement of composite properties via three-dimensional printing. *Mechanics of Advanced Materials and Structures*. 2019;(26):465–469. <https://doi.org/10.1080/15376494.2018.1432809>
27. Rosewitz J.A., Choshali H.A., Rahbar N. Bioinspired design of architected cement-polymer composites. *Cement and Concrete Composites*. 2019;(96):252-265. <https://doi.org/10.1016/j.cemconcomp.2018.12.010>
28. Katzer J., Szatkiewicz T. Effect of 3D printed spatial reinforcement on flexural characteristics of conventional mortar. *Materials*. 2020;(13):3133. <https://doi.org/10.3390/ma13143133>
29. Salazar B., Aghdasi P., Williams I.D., Ostertag C.P., Taylor H.K. Polymer lattice-reinforcement for enhancing ductility of concrete. *Materials & Design*. 2020;(196):109184. <https://doi.org/10.1016/j.matdes.2020.109184>
30. Liu Y., Zwingmann B., Schlaich M. Carbon fiber reinforced polymer for cable structures—a review. *Polymers*. 2015;(7):2078-2099. <https://doi.org/10.3390/polym7101501>
31. Wittbrodt B., Pearce J.M. The Effects of PLA Color on Material Properties of 3-D Printed Components. *Additive Manufacturing*. 2015;(8):110–116. <http://doi.org/10.1016/j.addma.2015.09.006>
32. Hasanzadeh A., Shooshpasha I. Effects of silica fume on cemented sand using ultrasonic pulse velocity. *Journal of Adhesion Science and Technology*. 2019;(33):1184–1200. <https://doi.org/10.1080/01694243.2019.1582890>
33. Hasanzadeh A., Shooshpasha I. Influence of silica fume on the geotechnical characteristics of cemented sand. *Geotechnical and Geological Engineering*. 2020;(38):6295–6312. <https://doi.org/10.1007/s10706-020-01436-w>
34. Chen Y., Matalkah F., Soroushian P., Weerasiri R., Balachandra A. Optimization of ultra-high performance concrete quantification of characteristic features. *Cogent Engineering*. 2019;(6):1558696. <https://doi.org/10.1080/23311916.2018.1558696>
35. Shihada S., Arafa M. Effects of silica fume ultrafine and mixing sequences on properties of ultra high performance concrete. *Asian Journal of Materials Science*. 2010;(2):137-146. <http://doi.org/10.3923/ajmskr.2010.137.146>
36. Zhang H., Cao C., Yilmaz E. Influence of 3D-printed polymer structures on dynamic splitting and crack propagation behavior of cementitious tailings backfill. *Construction and Building Materials*. 2022;(343):128137. <http://doi.org/10.1016/j.conbuildmat.2022.128137>
37. Mechtcherine V., Grafe J., Nerella V.N., Spaniol E., Hertel M., Füssel U. 3D-printed steel reinforcement for digital concrete construction — Manufacture mechanical properties and bond behaviour. *Construction and Building Materials*. 2018;(179):125-137. <https://doi.org/10.1016/j.conbuildmat.2018.05.202>
38. Le T.T., Austin S.A., Lim S., Buswell R.A., Law R., Gibb A.G.F., Thorpe T. Hardened properties of high-performance printing concrete. *Cement and Concrete Research*. 2012;(42):558–566. <https://doi.org/10.1016/j.cemconres.2011.12.003>
39. Xu Y., Zhang H., Gan Y., Šavija B. Cementitious composites reinforced with 3D printed functionally graded polymeric lattice structures: Experiments and modelling. *Additive Manufacturing*. 2021;(39):101887. <https://doi.org/10.1016/j.addma.2021.101887>